



This open access document is posted as a preprint in the Beilstein Archives at <https://doi.org/10.3762/bxiv.2021.63.v1> and is considered to be an early communication for feedback before peer review. Before citing this document, please check if a final, peer-reviewed version has been published.

This document is not formatted, has not undergone copyediting or typesetting, and may contain errors, unsubstantiated scientific claims or preliminary data.

Preprint Title Photothermal ablation of murine melanomas by Fe₃O₄ nanoparticle clusters

Authors Xue Wang, Lili Xuan and Ying Pan

Publication Date 08 Sep 2021

Article Type Full Research Paper

ORCID® iDs Ying Pan - <https://orcid.org/0000-0003-0262-8056>

Photothermal ablation of murine melanomas by Fe₃O₄ nanoparticle clusters

Xue Wang †¹, Lili Xuan †¹, Ying Pan *¹

Address:

¹Department of Obstetrics & Gynecology, China–Japan Union Hospital of Jilin University, Changchun, People's Republic of China.

Email:

Ying Pan - panying@jlu.edu.cn

* Corresponding author

‡ Equal contributors

Abstract

Melanoma is one of the deadliest forms of cancer, for which therapeutic regimens are usually limited by the development of resistance. Here, we fabricated the Fe₃O₄ nanoparticle clusters (NPCs) that have drawn widespread attention and investigated their role in the treatment of melanoma by photothermal therapy (PTT). Transmission electron microscopy imaging shows that our synthesized NPCs are spherically shaped with an averaged diameter of 329.2 nm. They are highly absorptive at the near-infrared 808 nm wavelength and efficient at converting light into local heat. *In vitro* experiments using light-field microscopy and MTT assay showed that Fe₃O₄ NPCs, in conjunction with near-infrared irradiation, effectively ablated A375 melanoma cells by inducing overt apoptosis. Consistently, *in vivo* studies using BALB/c mice found that intratumoral administration of Fe₃O₄ NPCs and concomitant *in situ* exposure to near-infrared light significantly inhibited growth of implanted tumor xenografts. Finally, we revealed, by experimental approaches including semi-quantitative PCR, western blot and immunohistochemistry, the heat shock protein HSP70 to be upregulated in response to PTT, suggesting this chaperone protein could be a plausible underlying mechanism for the observed therapeutic outcome. Altogether, our results highlight the promise of Fe₃O₄ NPCs as a new PTT option to treat melanoma.

Keywords

Fe₃O₄ nanoparticle clusters; heat shock protein 70; melanoma; near infrared; photothermal therapy

Introduction

The global incidence of melanoma, one of the deadliest forms of cancer, has kept increasing annually over the past decades at an accelerating rate [1]. Depending on the features of melanomas, therapeutic options include surgical resection, chemotherapy, immunotherapy, photodynamic therapy and several others. Although these treatments could initially meet therapeutic needs, their efficacies commonly drop afterwards due to adverse effects or development of various resistance mechanisms, making the advent of novel strategies imperative for early diagnosis and efficient treatment [2].

Photothermal therapy (PTT) is a recently developed regimen that requires administration of nanomaterials with unique optical properties to absorb and convert near-infrared (NIR) light into local heat [3]. Because nano-sized agents tend to accumulate within tumor site due to enhanced permeability and retention (EPR) effect, meanwhile tumor cells are more sensitive to elevated temperature than normal counterparts, PTT specifically ablates tumor cells, while leaving healthy neighbor tissues intact [4, 5]. Treatment specificity is further guaranteed by the high transmissivity and low absorption of NIR light when penetrating through biological tissues, making PTT a minimally invasive approach for tumor intervention.

One such type of nanomaterial that has received considerable attention is Fe₃O₄-core based nanoparticles, which have been approved by the Food and Drug Administration (FDA) as safe biomaterial with no long-term toxicity [6, 7]. The superparamagnetic properties make them ideally suited for many biomedical applications, such as MRI imaging, targeted drug delivery and biomolecule separation [8, 9]. *Yu et al* first

discovered strong photothermal effects of alumina-coated Fe₃O₄ nanoparticles against bacteria upon exposure to NIR light [10]. Further studies with esophageal cancer demonstrate that Fe₃O₄ nanoparticles induce hyperthermia post absorption to suppress tumor growth in a dosage-dependent manner [11]. However, due to extra-high-dosage needed to elicit sufficient hyperthermia by NIR irradiation, lingering magnetite may impose potential systemic toxicity. Thus, Fe₃O₄ single nanoparticles must be modified to reduce dosage regimen but meanwhile to keep their therapeutic efficacy. Recent findings show that clustered magnetic Fe₃O₄ nanoparticles induce a red-shift in the light absorption spectra, which enhances light absorbance within NIR region to improve their utilization as photosensitizers during PTT to ablate lung tumors [12]. However, the role of Fe₃O₄ nanoparticle clusters in the treatment of cutaneous melanoma has remained unknown.

In this study, we synthesized Fe₃O₄ superparamagnetic nanoparticle clusters, examined their morphology by scanning electron microscopy and tested their capacity of light-to-heat conversion. Then, we evaluated the effectiveness of the as-synthesized nano-clusters as PTT agents both *in vitro* and *in vivo*, and finally explored the putative molecular mechanisms underlying the observed therapeutic effects.

Results and Discussion

Properties of Fe₃O₄ nanoparticle clusters (NPCs)

The as-synthesized individual Fe₃O₄ nanoparticles were evenly dispersed in chloroform solution with high thermal stability. Transmission electron microscopy (TEM) revealed a typical face-centered cubic structure that was uniformly sized with an average diameter being 5.2 ± 1.5 nm (Figure 1a) [13]. After surfactant DTAB was

introduced, its lipophilic ends combined with the oleic acid and oleylamine ligands present on the surface of Fe_3O_4 nanoparticles through van der Waals force to facilitate the dispersion of nanoparticles in aqueous solution. Further addition of ethylene glycol weakened the van der Waals interaction, causing decomposition of nanoparticle micelles and the formation of Fe_3O_4 nanoparticle clusters, which were then coated with the polymers PVP to improve the nanoparticles' stability, biocompatibility and chemical features. Further interrogation by TEM revealed the as-formed Fe_3O_4 NPCs to be spherically shaped and uniformly sized with an average dimension of ~ 329.2 nm (Figure 1b). Moreover, TEM image at higher magnification showed the clusters were composed of many regularly organized small nanoparticles, preventing the loss of superparamagnetism due to increased particle size. These NPCs possess high magnetization with a saturation value of 59.4 emu/g (Figure 1c), stronger absorption intensities at the NIR 808 nm wavelength than individual nanoparticles [13]. Altogether, our data confirmed the successful fabrication of superparamagnetic Fe_3O_4 NPCs that are spherically shaped, uniformly sized and highly absorptive at NIR region, validating their potential use as PTT agents.

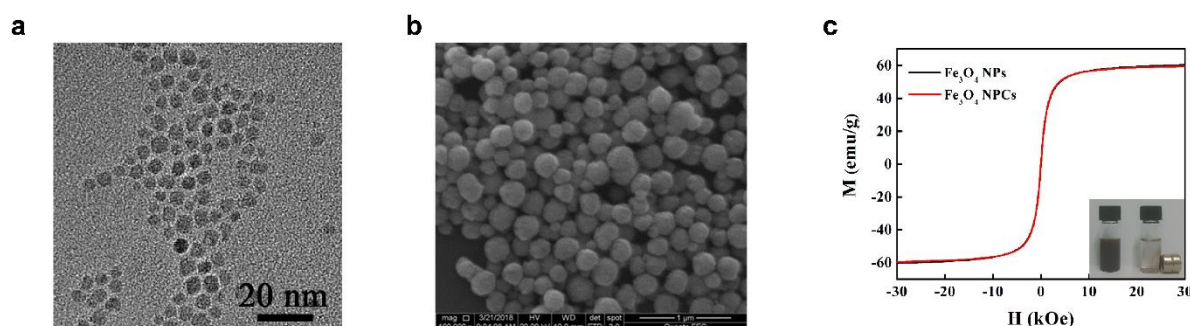


Figure 1: Characterization of the superparamagnetic Fe_3O_4 nanoparticle clusters. **a** Transmission electron microscopy (TEM) image revealing cubic morphology of individual Fe_3O_4 nanoparticles with a uniform diameter of ~ 5.2 nm. Scale bar, 20 nm. **b** TEM image of clustered Fe_3O_4 nanoparticles with an average diameter of ~ 329.2

nm. Scale bar, 1 μm . **c** Magnetic hysteresis curves of individual Fe_3O_4 nanoparticles as well as NPCs. The insert shows aggregation of NPCs dispersed in aqueous solution by a magnet.

Photothermal effect of Fe_3O_4 NPCs

To assess their photothermal effect, we measured the increments of temperature at different concentrations of Fe_3O_4 NPCs during the 10-min irradiation by 808 nm laser *in vitro*. In general, Fe_3O_4 NPCs-induced photothermal effect was dosage-dependent, because NPCs at higher concentrations performed markedly better than at lower ones (Figure 2a). Importantly, at concentrations as low as 0.0615 mg/ml, Fe_3O_4 NPCs rapidly and significantly raised aqueous temperature after NIR irradiation in only 1 minute at a power density of 1 W/cm^2 . This effect was time-dependent with longer irradiation causing higher temperature. Eventually, aqueous temperature was elevated from 24°C at baseline to 48.1°C at the end of irradiation, leading to a maximum net increment of 24.1°C. By contrast, only a modest increase of 10.2°C was observed for saline solution, validating the photothermal effect was mainly attributed to Fe_3O_4 NPCs. As expected, stronger power densities led to markedly higher temperatures (Figure 2b). Altogether, our results support a rapid and strong photothermal conversion capacity of Fe_3O_4 NPCs that carry beneficial potentials as photothermal agents.

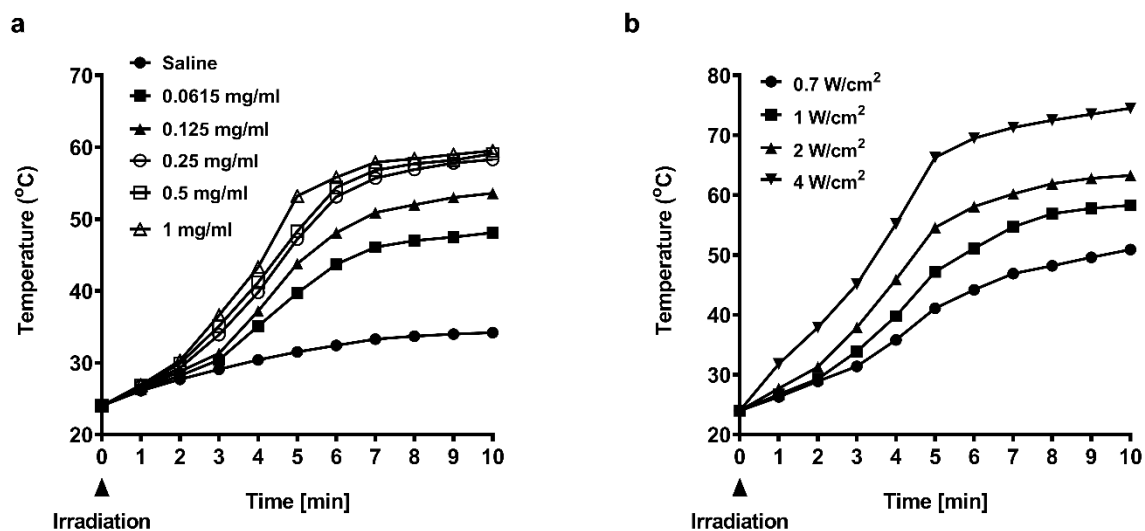


Figure 2: Photothermal conversion of Fe_3O_4 nanoparticle clusters. **a** Temperature elevation of aqueous solutions with increasing concentrations of NPCs in response to 808 nm laser irradiation at power density of 1 W/cm^2 . **b** Temperature elevation of solutions with 0.25 mg/ml NPCs in response to 808 nm laser irradiation at increasing power densities.

Photothermal ablation of tumor cells *in vitro*

To test their therapeutic effects *in vitro*, we first incubated A375 cells with increasing concentrations of Fe_3O_4 NPCs (0.0375 , 0.0625 , 0.125 , 0.25 mg/ml) or saline vehicle control, then treated them with or without NIR irradiation. Twenty-four hours later, light microscopy examination revealed that in the presence of NIR, NPCs caused overt apoptosis and necrosis in a dosage-dependent manner, which were manifested by morphological abnormalities, membrane segmentation and nuclei pyknosis (Figure 3a). The strongest effect was observed for the group using 0.25 mg/ml NPCs. NPCs alone, on the contrary, did not affect cell viability at low concentrations and only caused signs of mild cellular toxicity at high concentrations. Similarly, cells in the saline + NIR group seemed as healthy as those in the saline control group. Consistent with our

morphological observations, MTT viability assay showed that in combination with NIR irradiation, Fe₃O₄ NPCs led to significant cell death in a dosage-dependent manner, with the efficacious concentrations starting at as low as 0.625 mg/ml (Figure 3b). The strongest effect was observed for 0.25 mg/ml NPCs that, when compared to saline-alone control, reduced cell viability to 39.3%. NPCs alone tended to decrease cell viability at higher dosage but did not reach statistical significance, whereas cells exposed to saline + NIR remained unchanged. These findings indicated that our Fe₃O₄ NPCs possess high biocompatibility and are able to ablate melanoma cells at low concentrations under NIR irradiation.

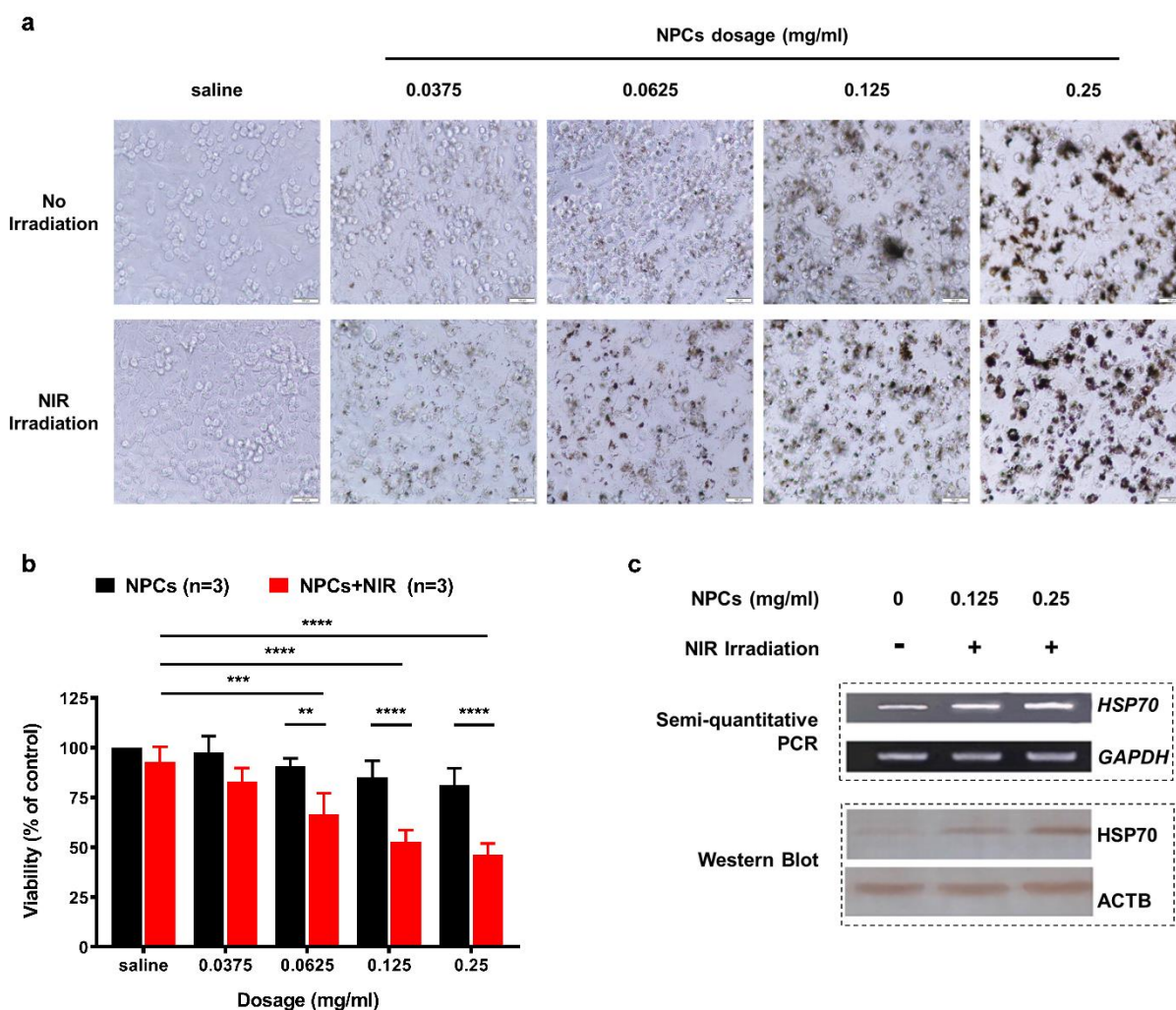


Figure 3: *In vitro* photothermal ablation of A375 cells. **a** Bright-field microscopy showing the health conditions of A375 cells treated with saline or increasing

concentrations of NPCs, in the presence or absence of NIR irradiation. **b** MTT assay showing viability of A375 cells after their incubation with NPCs at different concentrations with or without NIR exposure. ** $p < 0.01$, *** $p < 0.001$, **** $p < 0.0001$ calculated by two-way ANOVA adjusted by Sidak's multiple comparisons. **c** Expression of HSP70 in A375 cells was increased after treatment with NPCs (0.125 and 0.25 mg/ml) under NIR irradiation. This increase was observed on both mRNA and protein levels as revealed by semi-quantitative PCR and western blot, respectively.

HSP70 is frequently activated in response to heat stress and earlier studies have found it promotes apoptosis at least by eliciting antitumor immune responses [14]. To check whether HSP70 was involved in Fe₃O₄ NPCs mediated PTT, we treated A375 cells for 24 hours with NPCs at concentrations of 0.125 or 0.25 mg/mL, followed by 808-nm laser irradiation. Naïve cells were incubated with saline and served as normal controls. Then, we measured HSP70 expression by semi-quantitative RT-PCR and western blot, and found that expression of HSP70 was markedly increased on both mRNA and protein levels (Figure 3c), suggesting of a critical role it plays in mediating the as-observed therapeutic outcomes.

Photothermal ablation of tumor cells *in vivo*

To test their therapeutic efficacies *in vivo*, we first implanted A375 cells subcutaneously into BALB/c mice to form solid tumors. Then, they were randomly assigned into the five treatment groups as specified in the Experimental session. Briefly, these tumor-bearing mice were injected intratumorally with either Fe₃O₄ NPCs (2.5 mg/kg) or saline vehicle control, then exposed or not to NIR irradiation. Undisturbed BALB/c mice were maintained intact and served as normal control. Body weights, tumor volumes and general health conditions were monitored and recorded every other day over 8 days.

Our results found body weight of the normal control BALB/c mice rose steadily with a net final increment of 1.02 g (Figure 4a, b). In contrast, saline-alone group showed reduced body weight accompanied by a rapid growth of tumors that increased by 7.75-fold after 8 days (Figure 4c, d). Neither body weight nor tumor size was significantly different between saline + NIR and saline-alone groups, suggesting a negligible effect of NIR irradiation on biological tissues. Noticeably, we observed an initial drop of body weight in the NPCs-alone group during the first 4 days (Figure 4a), which implied our synthesized NPCs might possess light toxicity, a phenomenon echoed by our light microscopy findings (Figure 3a). In accordance, tumor volumes of this group were smaller than saline-alone group (Figure 4c, d). The quick restoration of body weight post day 4 demonstrated these materials are well tolerated and can be cleared out efficiently. Of importance, combination of NPCs with NIR irradiation dramatically shrank the tumors and reduced their volumes by 77.8% (Figure 4c, d). As a result, body weights of these PTT treated mice completely recovered after an initial drop by day 2 (Figure 4a), confirming feasibility of Fe₃O₄ NPCs as effective PTT agents. Finally, no abnormalities in general health status, defecation or urination were seen for all mice (data not shown).

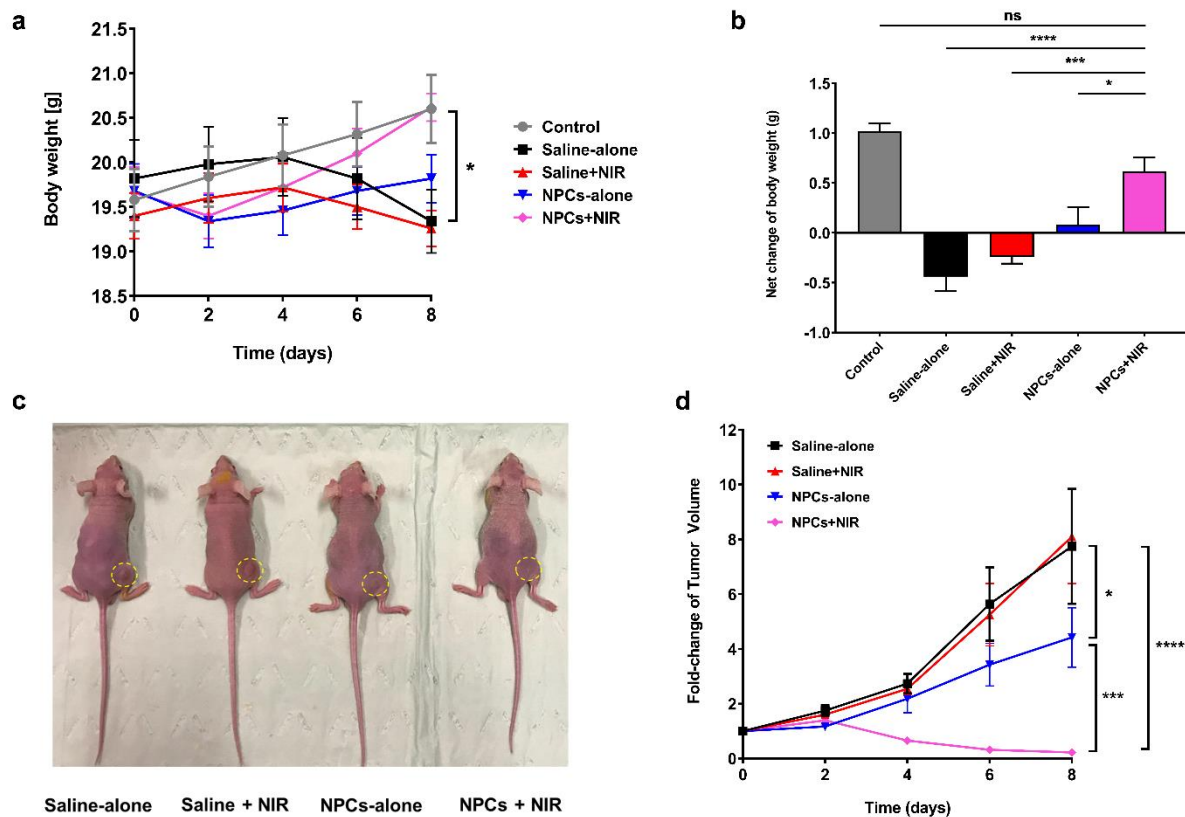


Figure 4: *In vivo* photothermal therapy in BALB/c mice bearing tumor xenografts. **a** Changes of body weight over the 8-day period post PTT. * $p < 0.05$, control vs NPCs + NIR at day-8, calculated by two-way repeated measures ANOVA adjusted by Tukey's multiple comparisons, $n = 8$. **b** Net body weight changes by the end of the study (day 8 versus day 0), * $p < 0.05$, *** $p < 0.001$, **** $p < 0.0001$ calculated by one-way ANOVA adjusted by Dunnett's multiple comparisons, $n = 8$. **c** Representative photographs of tumor-bearing mice in each treatment group by the end of the study. Yellow dashed circles indicate tumor location. **d** Growth curves of tumors in each treatment group. Tumor size was first normalized to its initial size (day-0), then expressed as fold-change over the latter. * $p < 0.05$, saline-alone vs NPCs-alone; *** $p < 0.001$, NPCs-alone vs NPCs + NIR; **** $p < 0.0001$, saline-alone vs NPCs + NIR; two-way repeated measures ANOVA adjusted by Tukey's multiple comparisons, $n = 8$.

To explore the molecular mechanisms underlying PTT, we performed immunohistochemistry to check tumoral HSP70 expression in saline-alone and NPCs + NIR groups. Similar to *in vitro* findings, the reduced tumor size was accompanied by markedly upregulation of HSP70 (Figure 5), confirming the involvement of HSP70 in Fe₃O₄ NPCs-mediated PTT *in vivo*.

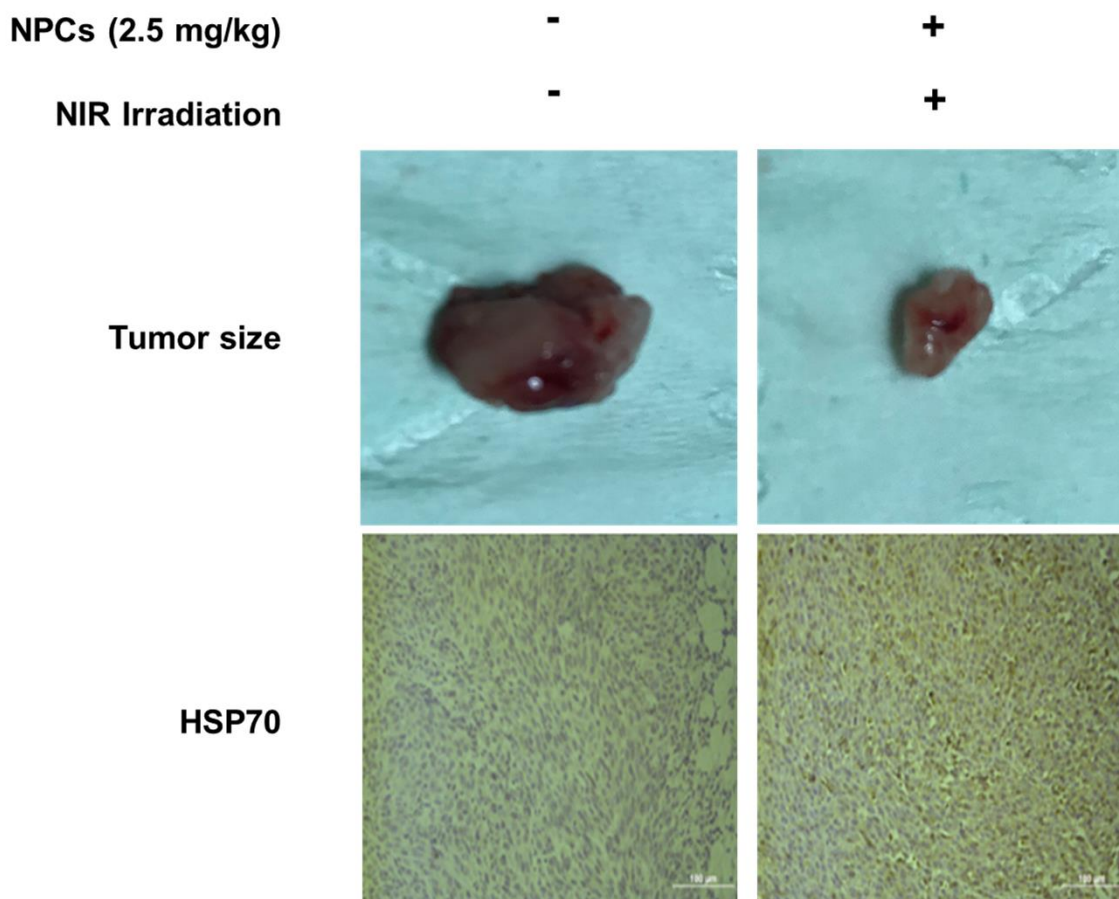


Figure 5: Photothermal therapy increases tumoral level of HSP70. Tumors were isolated from mice that received intratumor injection of either saline without NIR exposure or NPCs (2.5 mg/kg) followed by NIR irradiation. Immunohistochemical staining of harvested tumors revealed HSP70 to be elevated (brown signals) by PTT.

Conclusion

In summary, we fabricated Fe₃O₄ nanoparticle clusters that demonstrated uniformly shaped spherical structure, high absorption at near-infrared 808 nm wavelength, superparamagnetism and strong capacity of photothermal conversion. Both *in vitro* studies using immortalized A375 melanoma cell line and *in vivo* research using xenografted BALB/c mice model confirm these nano-clusters, under NIR irradiation, lead to overt cellular apoptosis and halt growth of implanted tumor xenografts at concentrations that do not elicit cytotoxicity when administered alone. Mechanistically, we discover the heat shock protein HSP70 as a plausible explanation for the observed therapeutic benefits as a result of hyperthermia. Findings of current study accentuate the potential application of Fe₃O₄ nanoparticle clusters in the treatment of melanoma.

Experimental

Reagents and Animals

Iron acetylacetonate (Fe (acac)₃, 99.9 +%), dibenzyl ether (99%), oleic acid (90%), oleylamine (> 70%), dodecyltrimethylammonium bromide (DTAB, 99%), tetradecyltrimethylammonium bromide (TTAB, 99%) and polyvinyl pyrrolidone (PVP, molecular weight 58,000) were purchased from Sigma-Aldrich. Decyltrimethylammonium bromide (DeTAB, 99%) and 1,2-hexadecanediol (97%) were purchased from TCI Chemical Industry Development Co., Ltd. (Shanghai). Chloroform (99%), ethylene glycol (96%) and ethanol (99.7%) were purchased from Beijing Chemical Works. Nitrogen gas was purchased from Juyang Gas (Changchun). Hela cells were purchased from the Cell Bank at Chinese Academy of Sciences (Shanghai, China). MTT (3-(4, 5-dimethylthiazol-2-yl)-2,5-diphenyltetrazolium bromide), penicillin/streptomycin and other biological reagents were purchased from

Sigma-Aldrich (St. Louis MO, USA). The BALB/c mice (7–8 weeks old) were provided by the Comparative Medicine Center of Yangzhou University. All animal experiments conducted in the current study were approved by the Institutional Animal Care and Use Committee (IACUC) of Jilin University (including guidelines for animal care, use, and euthanasia).

Synthesis of individual Fe₃O₄ nanoparticles

The Fe₃O₄ nanoparticles were synthesized via the thermal decomposition of precursor method as previously reported [15]. Specifically, under nitrogen atmosphere, a solution containing 0.01 mole 1,2 hexadecanediol and 20 ml dibenzyl ether was magnetically stirred within a three-necked flask (100ml). Then, 0.006 mole oleic acid, 0.006 mole oleylamine and 0.002 mole Fe (acac)₃ were added sequentially into that flask to mix up by continued stirring for 15 min. Next, the as-prepared mixture was gradually heated up to 200°C at a rate of 20°C/min and remained stirring for another hour at this temperature. Thereafter, the above-mentioned mixture was heated to and kept at 290°C for 1 hour in the presence of reflux stirring. After the solution was cooled down to room temperature, 50 ml of ethanol was added into the flask that was left on a strong magnet for 6 hours to collect the as-formed products. Finally, these products were washed three times with ethanol and dispersed in chloroform at a concentration of 1 mg/ml for later use.

Synthesis of clustered Fe₃O₄ nanoparticles

Step 1: PVP (0.58 g, molecular weight 58,000) was dissolved in 5 mL ethylene glycol under magnetic stirring. **Step 2:** DTAB or TTAB or DeTAB (0.02 g) were dissolved in 1 ml pure water, which was then combined with 10 mg individual ferric tetroxide (Fe₃O₄) nanoparticles in chloroform solution. **Step 3:** after 3 min vigorous vortex, the mixture in Step 2 was transferred into a three-necked flask that was incubated at 40°C in water bath when chloroform was repelled by nitrogen flow (this process takes about 3 min).

Step 4: The ethylene glycol solution from Step 1 was added into the mixture in Step 3 (add with a pipette gun, the time is controlled within 15 s) and mechanically stirred for 10 min at a rotation speed of 350 rad / min. Then, the resulting mixture in Step 4 was then heated to 80°C and maintained at that temperature for 6 hours. After cooling down to room temperature, the as-formed clusters were divided into two 10 ml centrifuge tubes, washed once with ethanol and centrifuged at 5000 rpm for 15 min to collect the final products that were dispersed in ethanol at a concentration of 20mg/ml. Morphologies of the as-synthesized nanoparticle clusters were characterized by JEOL JEM-2100 transmission electron microscopy (TEM).

Hyperthermia effect of Fe₃O₄ nanoparticle clusters in solution

The Fe₃O₄ nanoparticle clusters were diluted to various concentrations in saline (0.0375, 0.0625, 0.0125 or 0.25 mg/ml). One milliliter of each dilution was transferred into 10ml centrifuge tube and irradiated by 808-nm continuous-wave NIR laser (Changchun New Industries Optoelectronics Technology, Changchun, China) at power densities of 0.7, 1, 2 and 4 W/cm² with the spot size being 5 mm. Pre- and post-irradiation temperatures were recorded by a thermocouple positioned 1 cm beneath the solution surface. Measurements were made every 60 seconds over a 10 min time frame.

***In vitro* cytotoxicity assay**

A375 melanoma cell line was provided by the Core Laboratory at China–Japan Union Hospital of Jilin University. Use of this cell line was approved by the Animal Experimental Ethical Inspection Committee at Jilin University (Permit no.: 201802034). Cell culture was performed as previously described [16]. After reaching 70–80% confluence, they were seeded into 96-well plates at the density of 10⁴ cells per well and cultured for 24 hours, after which they were treated with Fe₃O₄ nanoparticle clusters at different concentrations (0, 0.0375, 0.0625, 0.0125 or 0.25 mg/ml) for 4

hours in the presence or absence of 808-NIR irradiation (power density of 1W/cm² for 1 min). After another 24 hours, cells were examined by light microscope and subjected to MTT assay as per the manufacturer's instructions. Optical absorbance was measured at 490 nm using a microplate reader. Cell viability was calculated as percentage of OD value of treatment group over that of the control group. All experiments were repeated three times.

Western blot

A375 cells were thawed and seeded in 6-well plate to equilibrate for 24 hours prior to experiments. Then, they were either left intact (as control) or treated for 4 hours with Fe₃O₄ nanoparticle clusters at concentrations of 0.125 or 0.25 mg/ml. Then, cells were irradiated with 808 nm NIR laser for 10 minutes at the power of 1 W. Twenty-four hours after continued culturing, whole cellular protein lysates were prepared by in-well scrapping in RIPA buffer supplemented with protease inhibitors (Roche), followed by centrifugation at 12,000g for 10 minutes at 4°C to save the supernatant. Protein concentrations were determined by the BCA Protein Assay Kit according to the manufacturer's instructions (Thermo Fisher). Western blot was performed as previously described with modifications [17]. Briefly, proteins were resolved by SDS-PAGE, transferred to nitrocellulose membranes and blocked with 5% non-fat milk for 1 hour at room temperature. After over-night incubation with anti-HSP70 primary antibody (Cell Signaling Technologies, #4872) or anti-ACTB (Cell Signaling Technologies, #4970) at 4°C, membranes were washed with 1xTBST for 3 times and incubated for 1 hour at room temperature with HRP-conjugated Goat anti-Rabbit secondary antibody (Thermo Scientific). Membranes were washed three times with 1xTBST and rinsed in H₂O₂/DAB substrate mixture until reaction proceeding to the desired intensity. Finally, membranes were washed in water, dried and photographed by ChemiDoc™ MP Imaging System (Bio-Rad). Densitometric quantification analysis

was performed using built-in Image Lab software. Relative expression levels were presented as ratios of band intensities of HSP70 over the internal control gene GAPDH.

Semi-quantitative Reverse Transcription-PCR (RT-PCR)

Treatments of A375 cells were identical to those mentioned above. Total RNAs were isolated via TRIzol method following vendor's manual (Invitrogen) and quantified by NanoDrop. After DNase I treatment (Roche), 1 µg RNA was reverse-transcribed to cDNA using HiScript II 1st Strand cDNA Synthesis Kit (Vazyme). Benchtop PCR was performed on a GeneAmp PCR System 9700 machine in a 50 µl reaction volume: 1x PCR buffer (with Mg²⁺), 0.2mM dNTP, 0.2 µM primers, 50 ng of template cDNA, and 0.5 µl of Platinum TaqDNA polymerase (Invitrogen). The cycling parameters used were as follows: initial 94 °C for 5 min, followed by 30 cycles of 94 °C for 30 s, 55°C for 30 s and 72 °C for 60 s, an additional extension at 72 °C for 7 min, and finally hold at 4 °C. The PCR products were resolved by electrophoresis using agarose gels supplemented with ethidium bromide. Images of bands were acquired by ChemiDoc™ MP Imaging System (Bio-Rad) and quantification was performed using the built-in Image Lab software. Relative expression levels were presented as ratios of band intensities of HSP70 over the internal control gene GAPDH. Primer sequences for *Hsp70* are: 5'- TTTTGGTCCTAAGAATCGTTCA-3' (forward) and 5'- ACACTTTCGGCTGTCTCCTTCA-3' (reverse), for *Gapdh* are 5'- GGGTGATGCTGGTGCTGAGTATGT-3' (forward) and 5'- AAGAATGGGTGTTGCTGTTGAAGTC-3' (reverse).

***In vivo* photothermal therapy**

A total number of 2x 10⁶ cultured A375 cells were resuspended in normal saline and injected subcutaneously at the dorsal side of right hind leg of BALB/c nude mice (averaged body weight 20 g), which were returned to their cages for 4 days until tumors

grew to at least 5 mm in diameter. Thereafter, these mice were anesthetized and injected intratumorally with Fe₃O₄ nanoparticle clusters (2.5 mg/kg body weight) or saline vehicle, then either left undisturbed or irradiated at the tumor site with 808 nm NIR laser for 10 minutes. This irradiation procedure was repeated 4 times at 12 hours interval, leading to the following treatment groups (n=8 per group): 1) saline-alone, 2) saline + NIR, 3) nanoparticle clusters-alone, 4) nanoparticle clusters + NIR. Naïve tumor-free BALB/c nude mice served as normal control. Body weight, tumor volume and abnormal behaviors were closely monitored during the study.

Immunohistochemistry

At the end of *in vivo* photothermal therapy, mice were euthanized and fixed with 4% paraformaldehyde via intracardiac perfusion. Tumors were then collected, sectioned and analyzed by immunohistochemistry to investigate expression of HSP70 according to a standard protocol [18]. Images were captured using a bright-light microscope (Olympus).

Statistical analyses

All the data were analyzed by GraphPad Prism 8.0 and expressed as mean ± SD. One-way ANOVA was applied for comparison among multiple groups, followed by *post hoc* test. Student *t* test (two-tailed) was used for comparison between two groups. All statistical differences with *p* values < 0.05 were considered significant.

Supporting Information

None

Acknowledgements

None

Funding

This study was supported by the Natural Science Foundation of Jilin Province (Grant No. 20190201205JC).

References

1. Leonardi, G.C., et al., *Cutaneous melanoma: From pathogenesis to therapy (Review)*. Int J Oncol, 2018. **52**(4): p. 1071-1080.
2. Domingues, B., et al., *Melanoma treatment in review*. Immunotargets Ther, 2018. **7**: p. 35-49.
3. Hirsch, L.R., et al., *Nanoshell-mediated near-infrared thermal therapy of tumors under magnetic resonance guidance*. Proc Natl Acad Sci U S A, 2003. **100**(23): p. 13549-54.
4. Huang, X., et al., *Plasmonic photothermal therapy (PPTT) using gold nanoparticles*. Lasers Med Sci, 2008. **23**(3): p. 217-28.
5. O'Neal, D.P., et al., *Photo-thermal tumor ablation in mice using near infrared-absorbing nanoparticles*. Cancer Lett, 2004. **209**(2): p. 171-6.
6. Bobo, D., et al., *Nanoparticle-Based Medicines: A Review of FDA-Approved Materials and Clinical Trials to Date*. Pharm Res, 2016. **33**(10): p. 2373-87.
7. Yuan, G., et al., *Biocompatible PEGylated Fe(3)O(4) nanoparticles as photothermal agents for near-infrared light modulated cancer therapy*. Int J Mol Sci, 2014. **15**(10): p. 18776-88.
8. Kievit, F.M. and M. Zhang, *Surface engineering of iron oxide nanoparticles for targeted cancer therapy*. Acc Chem Res, 2011. **44**(10): p. 853-62.

9. Laurent, S., et al., *Magnetic iron oxide nanoparticles: synthesis, stabilization, vectorization, physicochemical characterizations, and biological applications*. Chem Rev, 2008. **108**(6): p. 2064-110.
10. Yu, T.J., et al., *Multifunctional Fe₃O₄/alumina core/shell MNPs as photothermal agents for targeted hyperthermia of nosocomial and antibiotic-resistant bacteria*. Nanomedicine (Lond), 2011. **6**(8): p. 1353-63.
11. Chu, M., et al., *Near-infrared laser light mediated cancer therapy by photothermal effect of Fe₃O₄ magnetic nanoparticles*. Biomaterials, 2013. **34**(16): p. 4078-4088.
12. Shen, S., et al., *Magnetic nanoparticle clusters for photothermal therapy with near-infrared irradiation*. Biomaterials, 2015. **39**: p. 67-74.
13. Wang, X.H., et al., *Enhanced photothermal-photodynamic therapy for glioma based on near-infrared dye functionalized Fe₃O₄ superparticles*. Chemical Engineering Journal, 2020. **381**.
14. Vostakolaei, M.A., et al., *Hsp70 in cancer: A double agent in the battle between survival and death*. J Cell Physiol, 2020.
15. Sun, S., et al., *Monodisperse MFe₂O₄ (M = Fe, Co, Mn) nanoparticles*. J Am Chem Soc, 2004. **126**(1): p. 273-9.
16. Wang, X., et al., *Photothermal effects of NaYF₄:Yb,Er@PE₃@Fe₃O₄ superparamagnetic nanoprobe in the treatment of melanoma*. Int J Nanomedicine, 2019. **14**: p. 4319-4331.
17. Liu, Z., et al., *Regulation of Monocarboxylic Acid Transporter 1 Trafficking by the Canonical Wnt/beta-Catenin Pathway in Rat Brain Endothelial Cells Requires Cross-talk with Notch Signaling*. J Biol Chem, 2016. **291**(15): p. 8059-69.

18. Watson, A.S. and E.J. Soilleux, *Detection of p62 on Paraffin Sections by Immunohistochemistry*. Cold Spring Harb Protoc, 2015. **2015**(8): p. 756-60.